

Choi Figure 1. 1-D spatial profiles of the intensity (left) and the noise power (right) for a KTP-crystal OPA. Profiles of both the unamplified (empty squares) and the amplified (full squares) images are shown.

the same G . Also, we obtained improvement over $NF_{\eta} = 0.86$ dB for the detection setup alone, owing to optical pre-amplification. Finally, we get $NF_{amp} = (-0.2 \pm 0.6)$ dB which agrees, within the experimental error, with the intrinsic 0dB NF predicted for a PSA. Thus, our OPA performed noiseless image amplification.

In summary, our work shows that a phase-sensitive OPA can be successfully employed for enhancing the imaging of faint objects, adding to its classical advantages of time-gating and phase discrimination.

Acknowledgments

This work was supported in part by the U.S. Office of Naval Research.

References

1. C.M. Caves, "Quantum limits on noise in linear amplifiers," *Phys. Rev. D*, **26**, 1817 (1982).
2. J.A. Levenson, *et al.*, "Reduction of quantum-noise in optical parametric amplification," *J. Opt. Soc. Am. B*, **10**, 2233 (1993).
3. M.I. Kolobov and P. Kumar, "Sub-shot-noise microscopy: imaging of faint phase objects with squeezed light," *Opt. Lett.*, **18**, 849 (1993); A. Gatti, *et al.*, "Quantum entangled images," *Phys. Rev. Lett.*, **83**, 1763 (1999).
4. E. Lantz and F. Devaux, "Parametric amplification of images," *Quantum Semiclass. Opt.*, **9**, 279 (1997).
5. S.K. Choi, *et al.*, "Noiseless optical amplification of images," *Phys. Rev. Lett.*, **83**, 1938 (1999).

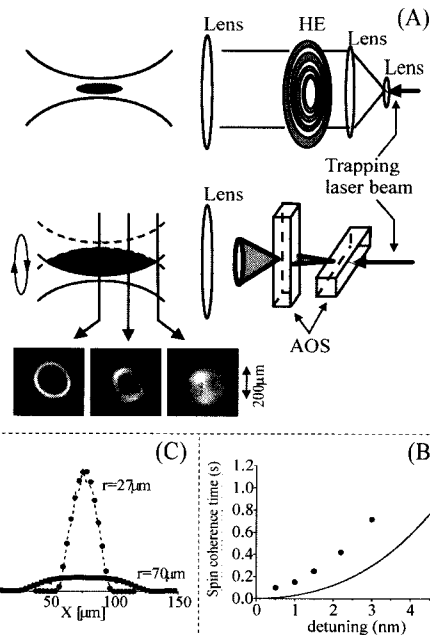
Single-Beam Dark Optical Traps for Cold Atoms

Nir Friedman, Lev Khaykovich, Roei Ozeri, and Nir Davidson

Cold atoms confined in far off-resonant optical dipole traps are useful for precision spectroscopy and for the study of quantum collective effects. To reduce interaction of the atoms with the trapping light, traps in which repulsive light forces confine atoms mostly in the dark were developed.¹ These dark optical traps enable long coherence times of the trapped atoms combined with tight confinement, and therefore high atomic densities. However, most schemes for dark optical traps require a combination of several laser beams, and this experimental complexity limits their wide use. Hence, single-beam dark traps are of great interest.

We have recently demonstrated single beam dark optical traps for cold atoms based on two different schemes (see Figure 1a). In the first scheme,^{2,3} the trap is formed using a holographic element (HE) that consists of equal-width rings, with a π radians phase difference between subsequent rings.⁴ When a beam that passes the HE is focused, destructive interference between adjacent rings ensures a dark region around the focus, which is surrounded by light in all directions.

The simplest HE, with only two phase rings, was used to



Friedman Figure 1a. Dark optical trap formed in two different schemes. Upper: using a binary phase holographic element (HE). Lower: using two perpendicular acousto-optic scanners (AOS). A dark volume completely surrounded by light is formed, as seen from the 3 measured light-intensity cross-sections along the trap. **1b.** Measured spin-coherence time, τ_{sc} , for atoms trapped in a two-rings HE dark trap, as a function of the trapping laser detuning. The full curve shows τ_{sc} calculated for the maximal light intensity, multiplied by a factor of 50, indicating the reduced interaction of the atoms with the trapping light. **1c.** Cross-sections of atoms trapped inside a rotating-beam dark trap, measured by absorption imaging. The trap was compressed from a radius of rotation of $70\mu\text{m}$ (●) to $27\mu\text{m}$ (○). The dashed curves present the results of Monte-Carlo simulations for the compression.

form a dark trap which had a 1:1000 light intensity ratio between the dark center and the surrounding ring. This trap was loaded with $\sim 10^5$ ^{85}Rb atoms, and stable trapping was achieved for a laser detuning as small as 0.1 nm above resonance. Long spin-coherence times of 100-1000 ms were measured (Figure 1b), indicating that the atoms were exposed on the average to as small as 1/700 of the maximal trapping light intensity.² A HE with a larger number of phase rings was also constructed, to produce a dark trap with a larger volume. 20 times more atoms were loaded into this trap, with even longer spin-coherence times.

In the second scheme, we used a rapidly rotating (up to 400 KHz) and tightly focused laser beam for the formation of a dynamic dark optical trap.⁵ The laser beam was rotated using two perpendicular acousto-optic scanners with a radius of rotation 2-6 times larger than the beam waist, so that a dark volume completely surrounded by light was obtained. We verified experimentally that for high rotation frequency the optical dipole potential can be precisely described by an effective time-averaged quasi-static potential. We demonstrated dynamic changes of the potential by trapping $> 10^6$ atoms in a large radius trap, and then adiabatically decreasing the rotation radius (Figure 1c). This compression resulted in a 350-fold increase in the atomic density, to a very high density of 5×10^{13} atoms/cm³, where an elastic collision rate of ~ 100 s⁻¹ was measured. A four-time adiabatic increase in the peak phase-space density was also obtained due to the change in the functional shape of the trap potential. The low interaction of atoms with the trapping light and the high

number of atoms and high density achieved make these optical traps very useful for spectroscopic research of cold atoms, and possibly for achieving quantum degeneracy.

Acknowledgment

This work was supported in part by the Israel Science Foundation and the Ministry of Science of Israel.

References

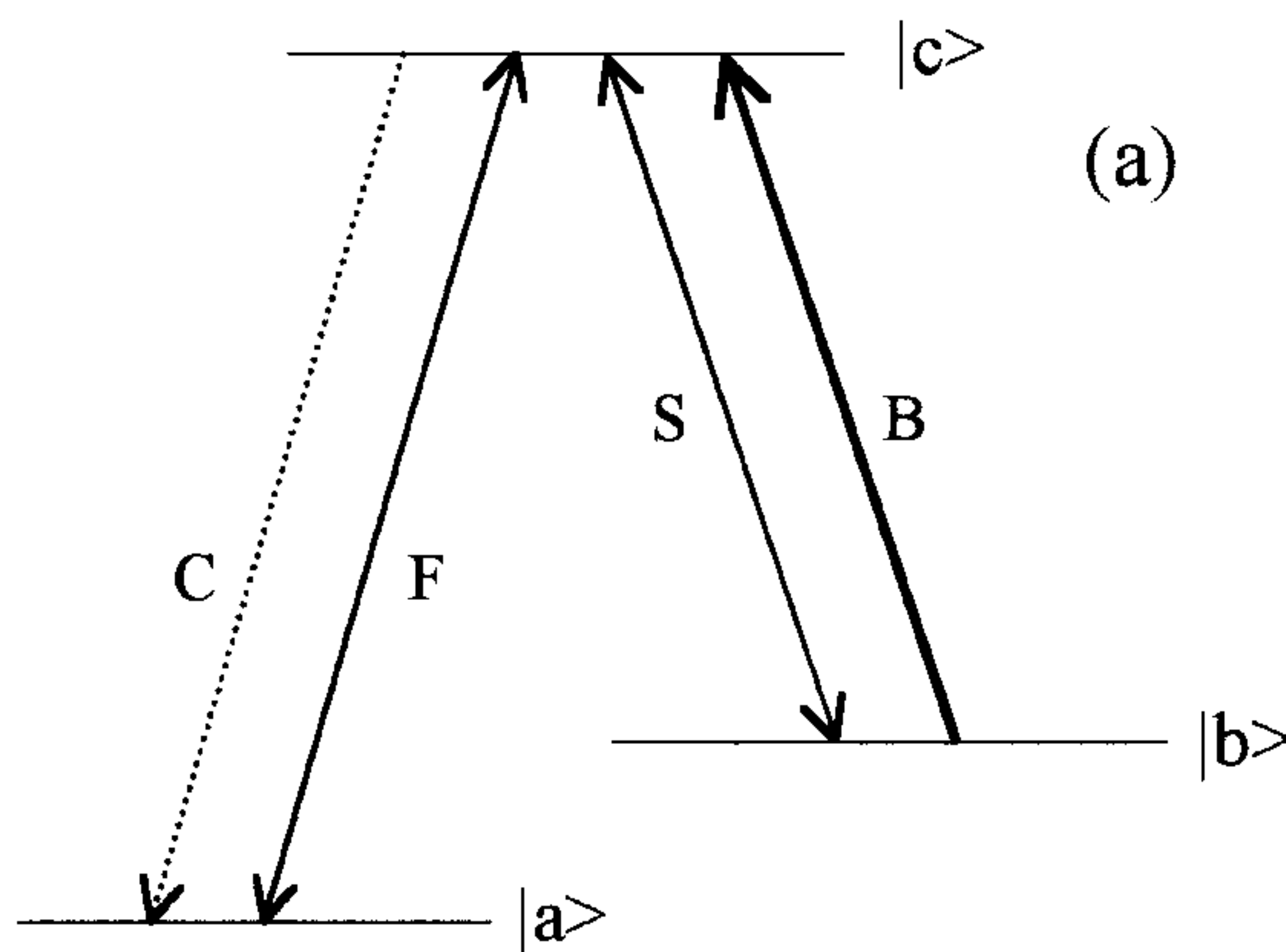
1. N. Davidson, *et al.*, "Long atomic coherence times in an optical dipole trap," *Phys. Rev. Lett.*, **74** (8), 1311 (1995).
2. R. Ozeri, *et al.*, "Long spin relaxation times in a single-beam blue-detuned optical trap," *Phys. Rev. A.*, **59** (3), R1750 (1999).
3. R. Ozeri, *et al.*, "Large volume single-beam dark optical trap for atoms using binary phase elements," *Rev. Sci. Instr.*, **70** (2), 1264 (1999).
4. N. Davidson, *et al.*, "Fabrication of binary phase surface relief optical elements by selective deposition of dielectric layers," *Rev. Sci. Instr.*, **70** (2), 1264 (1999).
5. L. Khaykovich, *et al.*, "Compression of cold atoms to very high densities in a novel rotating-beam blue-detuned optical dipole trap," Technical Digest QELS '99 (Baltimore, MD, 1999), QPD11-1.

Observation of Efficient Phase Conjugation Owing To Electromagnetically Induced Transparency in Solids

Byoung S. Ham and Philip R. Hemmer

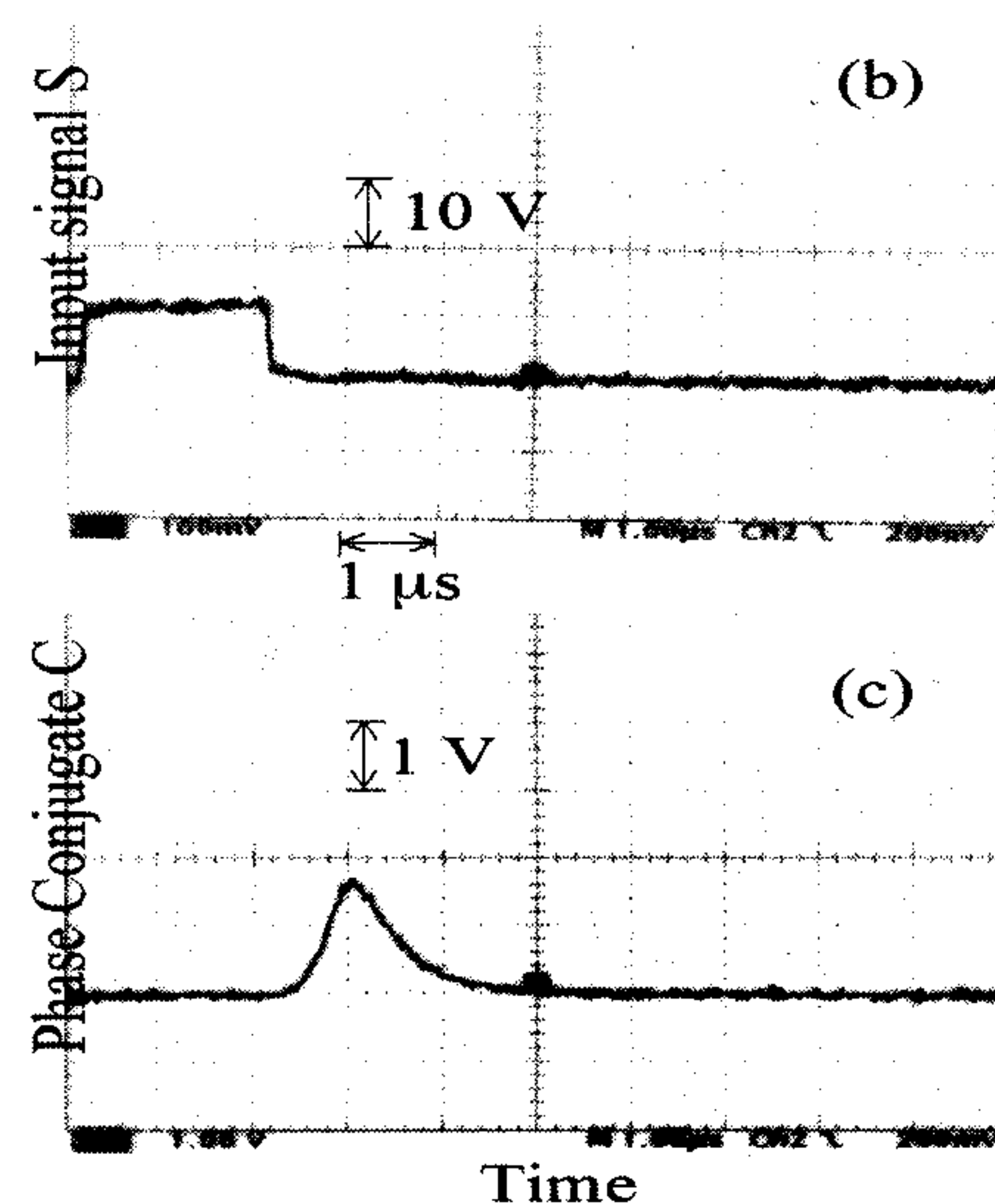
Since the first observation of electromagnetically induced transparency (EIT) in solids,¹ there have been many studies of its advantage for potential applications. Among them, enhancement of four-wave mixing generation is very useful for the implementation of potential EIT applications such as dynamic optical memories for THz fiber optic backbone networks and laser target tracking using turbulence aberration correction.² Of special interest is the recent observation of EIT above the critical temperature of a spectral hole-burning solid. This opens the door to applications of EIT in solids at higher temperatures than was possible previously.³ In the case of four-wave mixing in a Λ -type three-level system, frequency generation can be enhanced since the linear absorption is suppressed even at line center due to destructive quantum interference. Harris *et al.* proposed such an enhanced four-wave mixing system, and then Jain *et al.* demonstrated 40% conversion efficiency (power ratio of phase conjugate to input signal) using Pb vapors.⁴ Here it should be noted that Jain's experiment was based on near maximal Raman coherence using high-power pulsed lasers. Recently several research groups have demonstrated low-power, high-gain phase conjugation in atomic vapors. However, the conversion efficiency observed was less than 1%.

In this article we present the first observation of EIT enhanced phase conjugation in solids.⁵ The observed phase conjugate in $\text{Pr}^{3+}:\text{Y}_2\text{SiO}_5$ (Pr:YSO) is as high as ~22% of a backward pump power. Surprisingly, this was accomplished with a low power, unstabilized laser (frequency jitter ~80 MHz). Considering both that the laser jitter should degrade the Raman coherence and that the oscillator strength of Pr:YSO is as weak as ~1 millionth of that of atomic vapors, the observed phase conjugate in Pr:YSO is very efficient and suitable for the implementation of nonlinear optical processes such as optical memory and turbulence diagnostics.

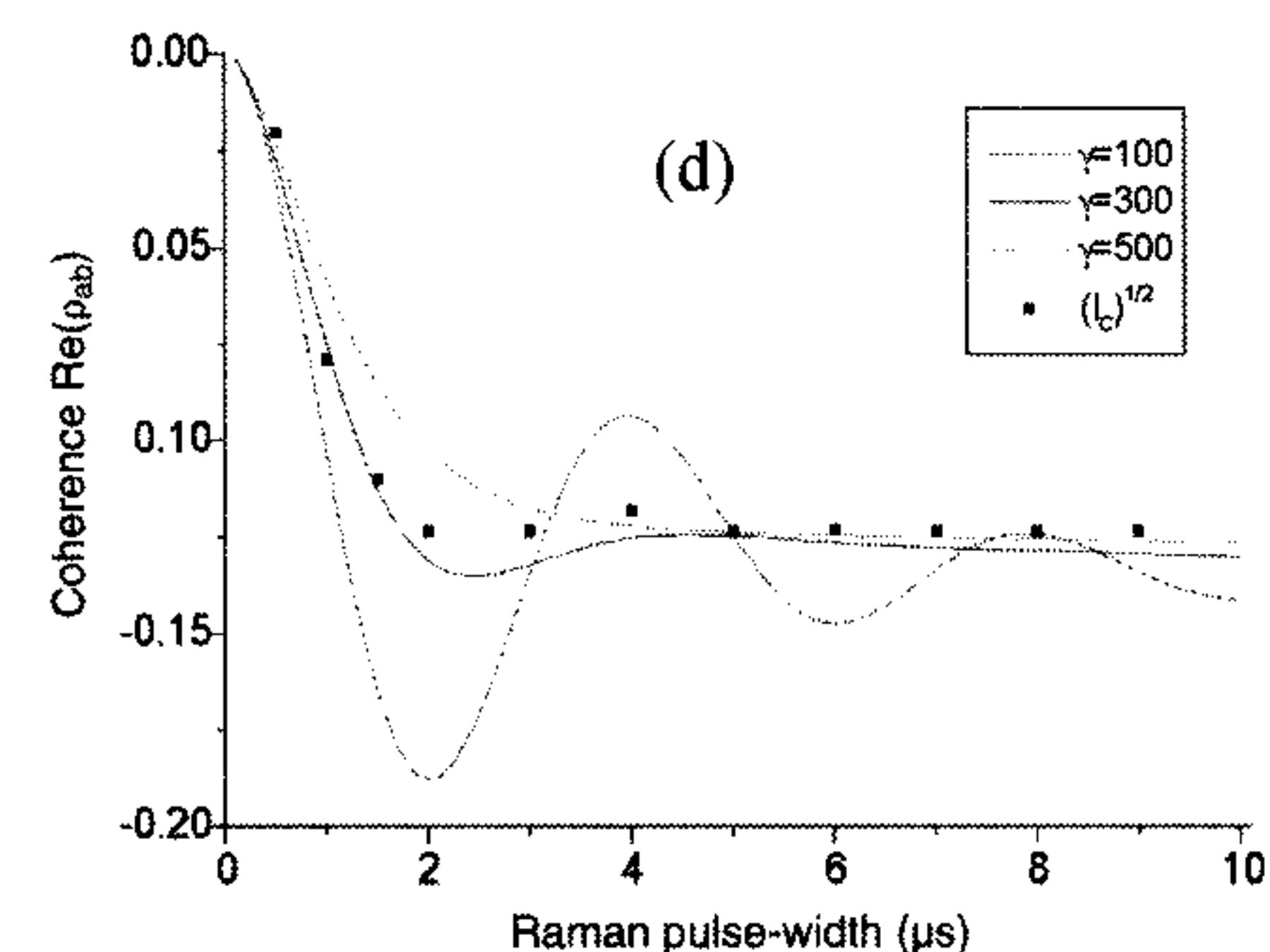


Ham Figure 1a. Energy-level diagram for phase conjugation owing to Raman coherence ρ_{ab} .

In Figure 1a, the optical transitions ($|a\rangle \leftrightarrow |c\rangle$ and $|b\rangle \leftrightarrow |c\rangle$) belong to the $^3\text{H}_4 \leftrightarrow ^1\text{D}_2$ manifold, which has a resonance frequency of ~606 nm. The phase-conjugate intensity I_C is proportional to the product of the square of the coherence ρ_{ab} and backward pump intensity I_B : $I_C \propto [\text{Re}(\rho_{ab})]^2 I_B$. The laser powers of F, S, and B are 6, 4, and 26 mW, respectively. To generate pulses, RF switches driven by a digital delay generator (Stanford DG 535) are used. The laser pulses F and S are concurrent and forward propagating with an angle of 80 mrad. The laser pulse B is backward propagating to the F and follows at the end of F and S. In Figure 1b and c, the input signal S and phase conjugate C, respectively, for individual pulses are shown. The peak voltage of the B is 65 V (not shown). Considering absorption coefficient ($\alpha = 10 \text{ cm}^{-1}$) and overlapping area (1/2) in the crystal, the frequency conversion efficiency is ~22% in peak power and ~10% in energy. We attribute this higher conversion efficiency to suppressed spectral hole burning, when the laser jitter exceeds the hyperfine splitting in the ground state of Pr:YSO. Figure 1d shows a simulation of the Raman pulse excited coherence $\text{Re}(\rho_{ab})$ for three different cases of the optical dephasing rate γ . Comparing the calculated conversion efficiency with the data, we conclude that the Raman induced coherence $\text{Re}(\rho_{ab})$ at $2\mu\text{s}$ is ~1/4 of the maximal coherence.



Ham Figure 1b and c. (b) Input signal S with attenuation by ND 2.0 and (c) phase conjugate C without attenuation.



Ham Figure 1d. Numerical simulation of the Raman induced coherence $\text{Re}(\rho_{ab})$: $\Omega_F=200$, $\Omega_S=160$, $\gamma_{\text{spin}}=0.5$, $\Gamma_{\text{spin}}=0$, and $\Delta_{\text{inh}}(|a\rangle \leftrightarrow |b\rangle)=25\text{kHz}$, where Ω , Γ , and γ are optical Rabi frequency, longitudinal decay rate, and transverse decay rate, respectively.